dione **4** (40 mg, 0.1 mmol) and ceric ammonium nitrate (5.6 g) was heated at reflux temperature in CH_3CN for 6 days. After water was added to the reaction mixture, CH_3CN was removed *in vacuo*, and the residue was extracted with ether. The organic extract was washed with water, dried over $MgSO_4$, concentrated *in vacuo*, and purified on SiO_2 (CH_2Cl_2) to give 25 mg of **5** (61% yield) as a crystalline solid: mp > 300 °C dec.; IR (KBr) 1660, 1640, 1580, 1280, 920 cm^{-1}; ^1H NMR ($CDCl_3$, 200 MHz) δ 7.35-7.51 (m, 16H, ArH); ^{13}C NMR ($CDCl_3$, 50.29 MHz) δ 129.22, 131.71, 138.39, 194.06; EIMS m/z (relative intensity) 416 (88, M^+), 388 (8), 296 (100), 268 (30); HRMS (EI) calcd for $C_{28}H_{16}O_4$ 416. 1046, found 416.1049.

8. Cho, S. J.; Hwang, H. S.; Park, J. M.; Oh, K. S.; Kim, K. S. *J. Am. Chem. Soc.* **1996**, *118*, 485
9. Dewar, M. J. S.; Thiel, W. *J. Am. Chem. Soc.* **1977**, *99*, 4899.
10. Dupuis, M.; Spangler, D.; Wendoloski, J. J. NRCC Software Catalog, Vol. 1, Program No. QG01 (GAMESS) (University of California, Berkeley, CA, 1980).
11. Baker, J. *J. Comput. Chem.* **1986**, *7*, 385.
12. Bondi, A. *J. Phys. Chem.* **1964**, *68*, 441.
13. van Gunsteren, W. F. *Protein Eng.* **1988**, *2*, 5.
14. (a) Wunz, T. P. *J. Comput. Chem.* **1992**, *13*, 667. (b) Orozco, M.; Luque, F. J. *J. Am. Chem. Soc.* **1995**, *117*, 1378.
15. Discover User Guide, version 95.0. San Diego: Biosym Technologies, 1995.

Transformation of Nanoparticle Magnetite Prepared in Homogeneous Aqueous Solution

Hojun Kang, Choong Sub Lee†, Don Kim, Young Soo Kang, and Yeong Il Kim*

Department of Chemistry, Pukyong National University, Pusan 608-737, Korea
†Department of Physics, Pukyong National University, Pusan 608-737, Korea
Received January 14, 1998

Recently nanoparticles of inorganic materials such as metal and semiconductor have been paid great attention due to the novel properties compared to their bulk materials.[1] Especially magnetic nanoparticles are of great interest for wide practical applications in information storage systems, catalysts, ferrofluids and medical diagnostics.[2] Among the several ultrafine magnetic particles many studies are devoted to nanoparticles of magnetite (Fe_3O_4) and maghemite (γ-Fe_2O_3). These iron oxides which have a size less than 10 nm were usually synthesized in various matrix materials such as polymers,[3] micelles,[4] vesicles[5] and bilayer lipid membrane.[6] They were also produced in homogeneous aqueous solution with very narrow size-distribution although the synthesis in an aqueous solution had been known to give larger particles.[7] In those studies the synthesized nanoparticle magnetites, however, are not characterized well whether they are magnetite or maghemite or the mixture of two. Magnetite can be oxidized to maghemite and the oxidation proceeds by a topotatic reaction where the crystal structure is maintained throughout. Therefore the distinction between magnetite and maghemite is hardly possible from diffraction data in the case of small particle where the peak broadening is serious. At elevated temperature the transformation of magnetite to haematite (α-Fe_2O_3) directly or *via* maghemite in air was studied in some details.[8] At room temperature micrometer-sized magnetite is usually known to be stable in air and its oxidation to maghemite proceeds at surface over years.[9] In the case of the particle whose size is less than 10 nm the surface components occupy significant parts of whole particle and diffusion pathway of oxygen is very short. The oxidation could be therefore significant. However, the oxidation of nanoparticle magnetite by air at room temperature has not been studied systematically yet.

In this communication we report the synthesis and transformation of nanoparticle Fe_3O_4 which is prepared in an aqueous homogeneous solution. Nanosized Fe_3O_4 has been prepared by dropping a solution mixture of $FeCl_3$ and $FeCl_2$ (molar ratio of Fe(III)/Fe(II)=1.97) in 0.4 M HCl slowly into 1.5 M NaOH solution while the resulting solution is vigorously stirred and the solution pH is kept to 11-12 by adding additional NaOH solution. After the iron mixture solution is all dropped the resulting suspension is kept stirred for 30 minutes. The precipitates are isolated using a magnet and transferred to deionized water. The suspension is centrifuged in 4000 rpm and washed again with deionized water. This procedure is repeated three times and finally washed with acetone. The resulting precipitates are dried in a vacuum for 5 hours at room temperature. All solutions are thoroughly deoxygenated by purging high purity N_2 for at least 30 minutes and the synthesis and all handling are done in N_2-filled globe box.

Figure 1 shows the transmission electron microscopy (TEM) picture of the synthesized magnetite particles. The particles look spherical and have pretty even sizes. The average particle size is estimated to about 7.0 ± 1.2 nm from measuring 100 particles in the picture. This size is slightly smaller than that of magnetite nanoparticle previously prepared with a similar method by one of authors.[7] Figure 2 (a)

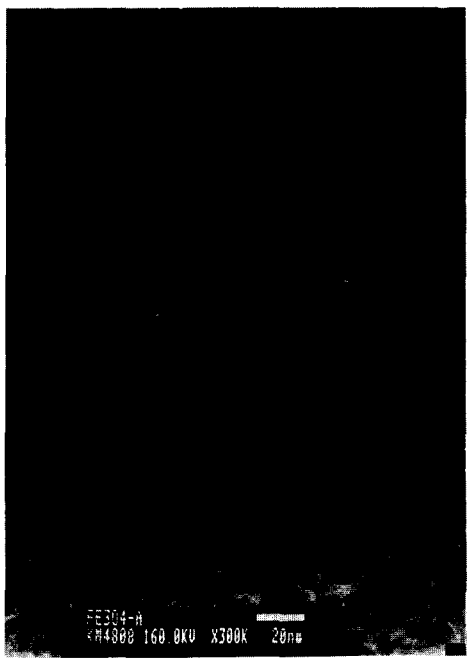

Figure 1. Transmission electron micrograph of synthesized magnetite particles.

shows XRD pattern of the magnetite sample immediately after synthesis. The data was corrected with background and smoothed because the signal-to-noise ratio was low due to small particle size and poor crystallinity. The discernible peaks can be indexed to (220), (311), (400), (511) and (440) planes of a cubic unit cell, which corresponds to that of magnetite or maghemite structure.[10] The unit cell parameter a_o is estimated as 8.3967 Å using Nelson-Riley extrapolation,[11] which is close to the known value of magnetite (8.387 Å).[12] We have also estimated the particle size of the synthesized ferrite from the linewidth as *ca* 8 nm using the Debye-Scherrer equation.[11] The calculated size is slightly larger than that from TEM picture but this is not unacceptable considering the reliability of Debye-Scherrer equation.

The XRD data can not confirm the structure of synthesized ferrite as magnetite or maghemite because maghemite also has a structure very similar to that of magnetite. In order to confirm the crystal phase of the synthesized ferrite we have sealed the sample immediately after synthesis in a quartz tube under vacuum (below 10 mtorr) and annealed it at 500 °C for an hour. If the sample is maghemite or it is a mixture of magnetite and maghemite, the XRD pattern will change to that of haematite (α-Fe_2O_3) or a mixture of magnetite and haematite because maghemite transforms to haematite at this temperature.[13] However, if the ferrite is pure magnetite, the XRD pattern will simply become sharp and intense because the crystallinity and particle size of the sample will increase without any phase transformation in this condition. The XRD peaks of the annealed sample are consisted of those of only magnetite and there is no discernible peak corresponding to those of haematite as shown in Figure 2(b). Therefore the synthesized ferrite is confirmed to be magnetite right after synthesis. However, we have found that the synthesized magnetite was oxidized by air at room temperature in the dry state and transformed to maghemite. Figure 3 shows the change of the ratio of Fe(II)/[Fe(II)+Fe(III)] in the magnetite exposed in air at room temperature with time. This is analyzed photometrically by dissolving the magnetite in acid solution and making phenanthroline complex.[14] The analysis was done very carefully in a N_2-filled globe box and all solutions were thoroughly deoxygenated before use. The amount of Fe^{2+} in the ferrite relatively quickly decreased in initial three days and then very slowly decreased. Figures 4(a) and 5(a) show the XRD patterns of aged magnetite nanoparticles in air at room temperature for 2 weeks and 3 months, respectively. In these XRD data no difference can be observed between fresh sam-

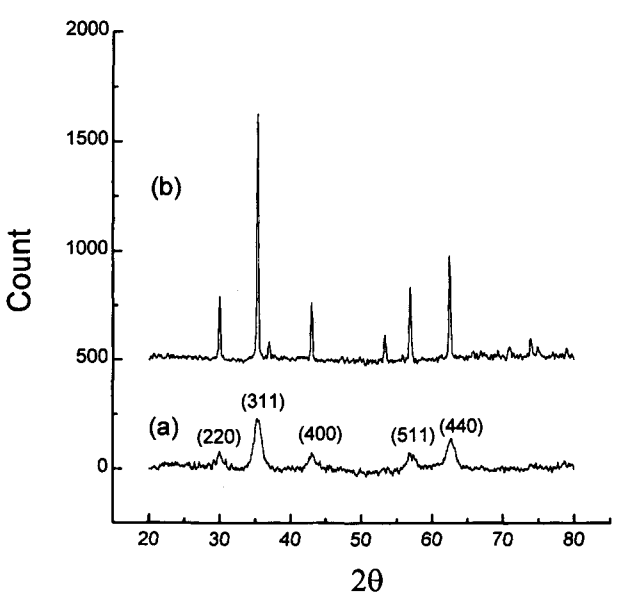

Figure 2. XRD patterns of nanoparticle magnetite right after synthesis: (a) as is and (b) annealed one under vacuum at 500 °C.

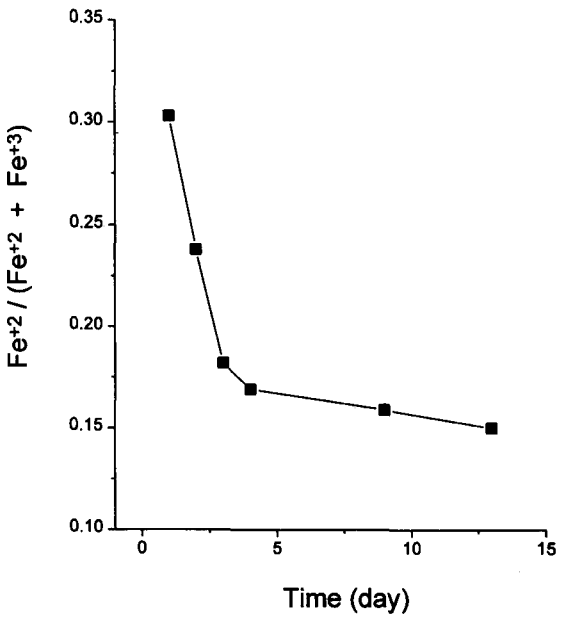

Figure 3. Change in degree of oxidation of magnetite nanoparticle with time.

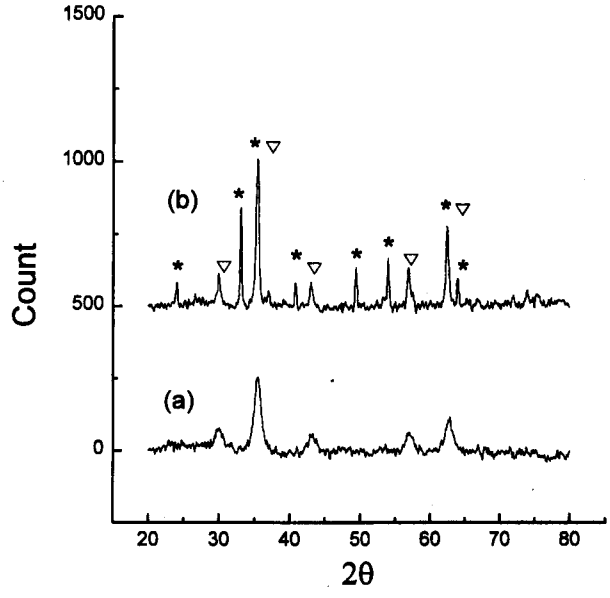

Figure 4. XRD patterns of nanoparticle magnetite exposed to air for two weeks after synthesis: (a) as is and (b) annealed one under vacuum at 500 °C.

ple (Figure 2(a)) and aged ones in air. Therefore we can not tell transformation of magnetite shown in bulk analysis from XRD patterns. This is because Fe_3O_4 and γ-Fe_2O_3 is structurally isotropic as mentioned above and the very small changes in diffraction peaks can be within the range of experimental error especially in nanoparticles where peak broadening is significant. In order to confirm the change of crystal phase we have annealed the aged samples which were exposed in air at room temperature for two weeks and three months after synthesis, at 500 °C in a vacuum. The results are shown in Figures 4(b) and 5(b). The XRD pattern of 2 week-aged sample corresponds to that of a mixture of magnetite and haematite whereas the pattern of 3 months-aged one does to that of almost haematite. As discussed above, the result on the sample that was annealed right after synthesis clearly indicates that maghemite phase must be formed in the aged samples. Therefore the oxidation of nanoparticle magnetite to maghemite proceeds in air at room temperature and the whole particle could be changed to maghemite.

We have also measured Mossbauer spectrum that is known to give a good criterion for quantitative analysis of iron oxide mixtures.[15] Figure 6 show the Mossbauer spectra of annealed samples immediately, 2 weeks and 3 months after synthesis.[16] The spectrum of fresh sample (A) was deconvoluted to two sextets that correspond to iron ions in tetrahedral (T_d) and octahedral (O_h) sites of magnetite. From the peak area ratio of two sextet peaks (I_{Oh}/I_{Td}=1.97) the sample was confirmed to be in pure magnetite phase. In the cases of 2 week-aged (B) and 3 month-aged (C) samples each spectrum was deconvoluted to three sets of sextet where one corresponds to peaks of haematite and the others to that of magnetite. From those relative peak area ratio we have estimated the relative molar ratio of haematite *vs* magnetite in the sample as 1.05 and 2.28 for sample B and C, respectively. This relative ratio for sample B is lower than the vaule 1.9 obtained from the wet analysis shown in Figure 2. The difference could result partly from the fact that the peak area value in Mössbauer spectrum corresponding to magnetite could include that of maghemite because the ratio I_{Oh}/I_{Td} (=1.66) is much lower than the ideal value 2 and the spectrum of maghemite is identical with that of tetrahedral sites in magnetite. This means that maghemite phase in sample B did not transform to hematite completely at this annealing condition. This can be applied to the case of sample C where the ratio I_{Oh}/I_{Td} is 1.55.

In summary we have prepared nanoparticle Fe_3O_4 which has an average diameter of 7 nm in homogeneous aqueous

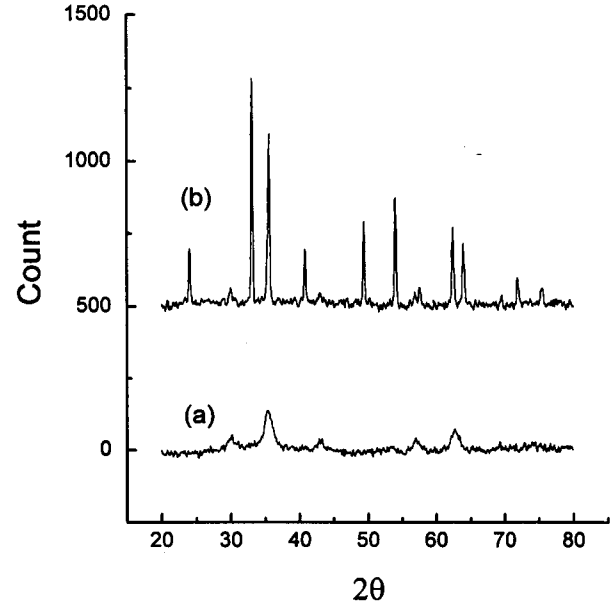

Figure 5. XRD patterns of nanoparticle magnetite exposed to air for three months after synthesis: (a) as is and (b) annealed one under vacuum at 500 °C.

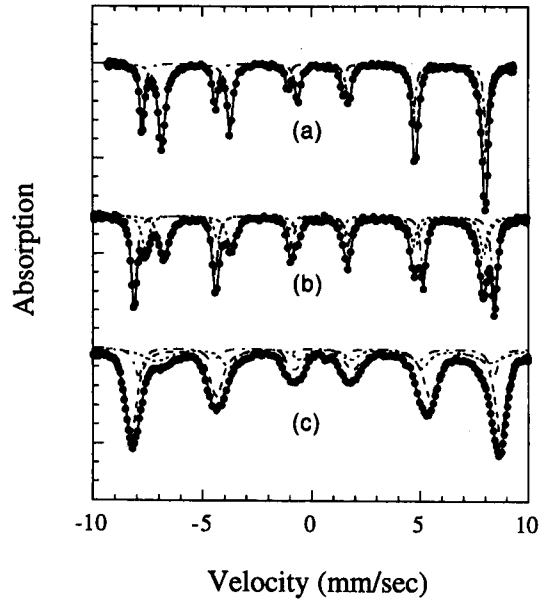

Figure 6. Mössbauer spectra of annealed magnetite nanoparticles. (a) right after synthesis and exposed to air (b) for 2 weeks and (c) 3 months after synthesis.

solution and clearly elucidated for the first time that the synthetic nanometer-sized magnetite was transformed to γ-Fe_2O_3 in air at room temperature by relatively fast oxidation. Therefore the previous studies of nanoparticle magnetites where the air oxidation was not considered have to be reconsidered in their characterization of the nanoparticles. In forthcoming papers we will investigate the size effect on the transformation and detailed studies of magnetic properties of nanoparticle magnetite under transformation to maghemite.

Acknowledgment. This work is supported by Basic Science Research Institution Program of Ministry of Education (BSRI-96-2455).

References

1. Henglein, A. *Chem. Rev.* **1989**, *89*, 1861.
2. *Science and Technology of Nanostructured Magnetic Materials*; Hadjipanayis G. C.; Prinz, G. A., Eds; Plenum: New York, 1991.
3. (a) Ziolo, R. F.; Giannelis, E. P.; Weinstein, B. A.; O'Horo, M. P.; Ganguly, B. N.; Mehrotra, V.; Russell, M. W.; Huffman, D. R. *Science* **1992**, *257*, 219. (b) Butterworth, M. D.; Armes, S. P.; Simpson, A. W. *J. Chem. Soc., Chem. Commun.* **1994**, 2129. (c) Sohn, B. H.; Cohen, R. E. *Chem. Mater.* **1997**, *9*, 264.
4. (a) Kommareddi, N. S.; Tata, M.; John, V. T.; McPherson, G. L.; Herman, M. F.; Lee, Y.-S.; O'Connor, C. J.; Akkara, J. A.; Kaplan, D. L. *Chem. Mater.* **1996**, *8*, 801. (b) Davies, K. J.; Wells, S.; Charles, S. W. *J. Magn. Magn. Mater.* **1993**, *122*, 24.
5. Mann, S.; Sparks, H. C.; Board, R. G. *Adv. Microb. Physiol.* **1990**, *31*, 125.
6. Zhao, X. K.; Herve, P. J.; Fendler, J. H. *J. Phys. Chem.* **1989**, *93*, 908
7. Kang, Y. S.; Risbud, S.; Rabolt, J. F; Stroeve, P. *Chem. Mater.* **1996**, *8*, 2209.
8. Gillot, B.; Rousset, A.; Dupre, G. *J. Solid. State Chem.* **1978**, *25*, 263.
9. Murad, E.; Schwertmann, U. *Clays Clay Min.* **1993**, *41*, 111.
10. Cornell, R. M.; Schwertmann U. *The Iron Oxides*; VCH: New York, 1996, p 167.
11. Azaroff, L. B. *The Powder Method*; MacGraw Hill: New York, 1958.
12. JCPDS (Joint Committee on Powder Diffraction Standards) data base 19-629.
13. (a) Feitknecht, W.; Mannweiler, U. *Helv. Chim. Acta* **1967**, *50*, 570. (b) Egger, K.; Feitknecht, W. *Helv. Chim. Acta* **1962**, *45*, 2042.
14. Sandell, E. B.; Onishi, H. *Photometric Determination of Traces of Metals*; John Wiley: New York, 1978; p 367.
15. May, L. *An Introduction to Mossbauer Spectroscopy*; Plenum: New York, 1971.
16. Detail experimental procedures are described elsewhere.[17]
17. Kim, D.; Lee, C. S.; Kim, Y. I. *Bull. Korean Chem. Soc.* **1998**, *19*, In press.

Design and Synthesis of Amidine and Diphenyl Substituted Chiral Bispyridino-18-Crown-6 Ligands

Hongsuk Suh*, Jae-Kon Kim, In-Sun Jung, Sung-Eun Lee, Shin Won Kang, and Jang-Su Park

Department of Chemistry, Pusan National University, Pusan 609-735, Korea
Received January 15, 1998

Enantiomeric recognition phenomena play an important role in a variety of physical, chemical, and biological process. Examples include sensing, determination of concentrations, separations of enantiomers, catalysis reactions, and incorporation of single enantiomeric forms of amino acids and sugars in biochemical pathways. It involves the discrimination between enantiomers of the guest by a chiral receptor or a chiral matrix. One area of recent interest is the enantiomeric recognition through interaction of macrocyclic ligands with chiral organic ammonium salts.[1-4]

Several research groups have carried out works involving these host-guest systems. Cram and his co-workers published their pioneering studies on the use of chiral macrocyclic ligands in enantiomeric recognition and a great number of chiral macrocycles have been synthesized and studied.[5] Izatt and his co-workers have reported chiral recognition of primary aromatic ammonium salts.[6] Echavarren and his co-workers have studied enantiomeric recognition of zwitter ionic hydrogen bonding of carboxylate and guanidine.[7]

The careful characterization of such synthetic systems could lead to a greatly improved understanding of natural systems.

Our research in this field has been focused on the design and synthesis of amidine and diaryl substituted chiral bispyridino-18-crown-6 ligand. The chiral host molecule should be designed in such a way that the interaction options available for the incoming chiral guest are limited. Preferably, the options would be limited to either "match" or "not match" interactions (Figure 1).

Designed synthetic chiral ligands have two hydrogen bonding donor which can interact with the carboxylate of